The characterization of MnO nanostructures synthesized using the chemical bath deposition method

LF Koao[1], F B Dejene[1*] and HC Swart[2]

[1]Department of Physics, University of the Free State (Qwaqwa Campus), Private Bag X13, Phuthaditjhaba, 9866, South Africa
[2]Department of Physics, University of the Free State, P.O. Box 339, Bloemfontein, 9300, South Africa.

*Corresponding author: Tel: +27 58 718 5307; Fax: +27 58 718 5444; E-mail: dejenebf@ufs.ac.za

Abstract. Manganese oxide (MnO) nanoparticles were synthesized by the chemical bath deposition method. The pH of the solution was varied during the deposition process to determine the effect thereof. The temperature of the bath was maintained at 80^0C. The final yields were characterized for structural, morphology and luminescence properties. The X-ray diffraction spectrum of the MnO nanoparticles was monoclinic. The particle size was found to be dependent on the pH. Scanning electron microscopy micrographs depict irregular nanoparticles at low pH and flakes-like nanoparticles structures at a higher pH. Fourier transformed infrared spectroscopy analyses confirmed these MnO compositions. Photoluminescence spectra indicated that the nanoparticles product had emission peaks at 364, 381, 415 and 452 nm. The sample which was obtained at a pH of 9.01 has the broadest luminescent peak.

1. Introduction

It is well known that the synthesis of semiconductors nanostructures has attracted much attention in materials science for several years. Nanostructures can be used in microelectronic, electronic, optical and magnetic devices [1-2]. Manganese oxide (MnO) is also of interest due to its wide band gap (7.8 eV). It is semiconductor that can be used as optical window in optoelectronic devices and luminescent materials [3]. MnO nanostructure can easily be incorporated into polymer, glassy matrices where they can be applicable in fiber optics telecommunication [4] and the structures can also be incorporated in semiconductor nanoparticles (e.g. ZnO and ZnS) where they can be applied in light emitting diodes, laser diodes and ultraviolet photodetectors [4]. The optical property of the materials is related to its size and morphology, which encourage us to synthesize nanostructured MnO. The chemical bath deposition (CBD) is a simple, cheap and convenient process to prepare semiconducting materials. The more recent interest in all things 'nano' has also provided a boost for CBD, since it is a low temperature, solution (almost always aqueous) technique, crystal size is often very small. The aim of this paper is to investigate the effect of pH on the material properties of MnO.

2. Experimental

The MnO nanostructures were synthesized using the CBD process by varying the pH of the solution. The chemicals used for the preparation of the nano-powders were of analytical grade, which includes manganese acetate (Mn $(CH_3COO)_2.4H_2O$), Thiourea ($(NH_2)_2CS$) and Ammonia (25% NH_3). During the preparation of the nano-powders, the ammonia solution was used as a complexing agent. The temperature of the bath was kept constant at 80^oC. The precipitates were filtered and washed with ethanol and later dried at ambient conditions for several days. The particle size and morphology and the structural and luminescent properties of the as-synthesized phosphors were examined by means of

scanning electron microscopy (SEM), X-ray diffraction (XRD), Fourier transformed infrared spectroscopy (FTIR), X-ray photoelectron spectrometry (XPS) and Photoluminescence (PL).

3. Results and Discussion

3.1 Structural analysis and Composition analysis

The X-ray diffraction patterns of the MnO samples prepared at fixed manganese acetate to thiourea mole ratio of 1:1 but at different pH are shown in figure 1. All diffraction peaks at low pH of 7.73 could be indexed to the monoclinic MnO structure (JCPDS Number 39-1218). No characteristic peaks of any other impurities such as $Mn(OH)_2$ or precursors used are observed, indicating the formation of a pure phase of MnO. Further increase in pH to 9.01 does not affect the structure of the MnO phase. The broadness of the diffraction peaks indicates the presence of nanocrystallites in the MnO structures.

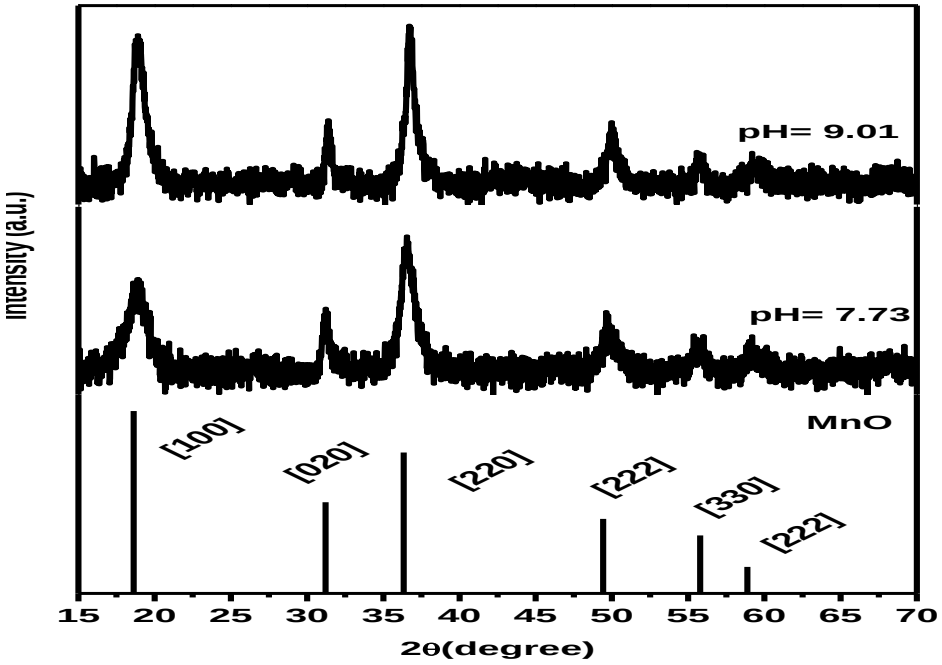

Figure 1. X-ray powder diffraction patterns for MnO prepared at different pH values.

The average size of the as-prepared nanocrystals can be calculated from the Full Width Half Maximum (FWHM) of the diffraction peaks using the Debye-Scherrer formula [5]. All major diffraction peaks for all samples are chosen to estimate the average size of the nanocrystals by the least square method. The estimated particle sizes were 28 and 44 nm for pH of 7.7 and 9.01, respectively. It is clear that the average particle size increased as the pH increased. The sizes of the products were found to be affected by the precursor concentration and synthesis time.

3.2 Surface morphological analysis

SEM micrographs of MnO prepared at low (7.74) and high (9.01) pH shown in figure 2, depict that the powders consisted out of agglomerated fluffy (flake-like) particles which contained nanocrystalites according to the XRD spectra. In comparing the SEM micrographs it is clear that at the high pH value the nanostructures are less agglomerated. The flakes-like appearance is more pronounced at the high pH value.

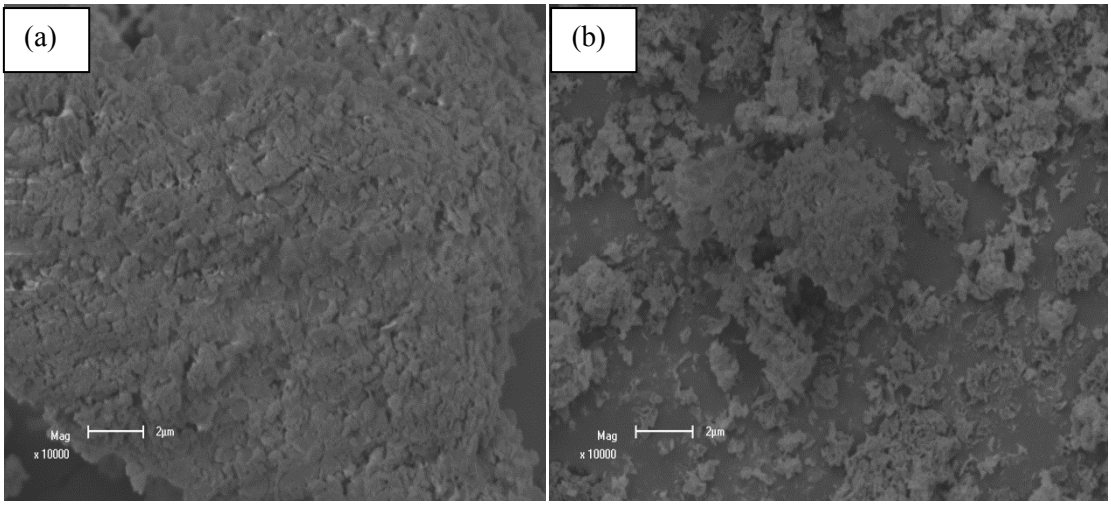

Figure 2. SEM images of MnO nanostructures as synthesized at pH values of (a) 7.74 and (b) 9.01.

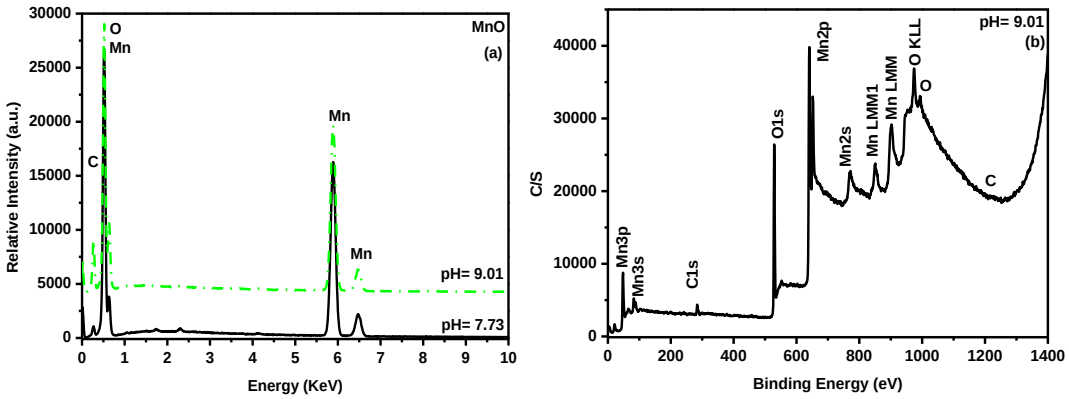

Figure 3. Representative (a) EDX and (b) XPS spectra of the MnO nanocrystals prepared at different pH values.

The elemental analysis and purity of the MnO samples were analysed using EDS and XPS. The EDS spectra in Figure 3(a) show the presence of Mn and O for all the samples. The pH does not have significant effect on the EDS spectra. The existence of C (carbon) is originating from the double sided carbon tape. The stub (sample holder) was covered with double sided carbon tape so that the powder samples can easily be adhered to avoid the sample from falling. XPS results in figure 3(b) shows the survey spectrum of the MnO nanoflakes-like structures prepared at a pH solution of 9.01. Mn, O and C were present. The peaks located at 47, 77, 642, 768, 849 and 902 eV are assigned to the binding energies of Mn_{3p}, Mn_{3s}, Mn_{2p}, Mn_{2s}, Mn_{LMM1} and Mn_{LMM}, respectively; and those at 530 and 973 eV are ascribed to the binding energies of O_{1s} and O_{KLL}. All of the observed binding energy values for Mn and O are consistent with the data reported in the literature [6]. The existence of C impurity in the XPS results is believed to have originated from the surface contamination in the atmosphere and the C tape. Both EDS and XPS measurements indicate that MnO nanostructures obtained were pure.

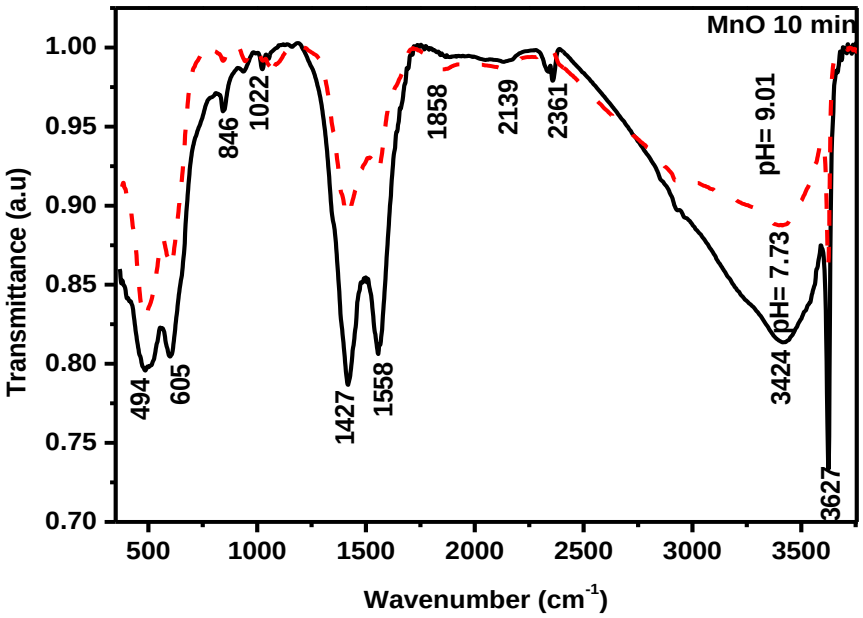

Figure 4. Representative FTIR spectra of the MnO nanocrystals prepared at different pH values.

Figure 4 represents the FTIR spectra recorded for the MnO nanostructures in the range of 350 cm^{-1} to 4500 cm^{-1}. IR spectral analyses allowed us to investigate the bonding type and further elucidate the identity of the products. MnO has been reported to display a single peak at around 626 with a broad peak between 400-600cm^{-1} [7]. The broad absorption peaks at 3424 and 1427 cm^{-1} are attributed to the stretching and bending vibration of hydroxyl, respectively [8]. The narrow band at around 3627 cm^{-1} is assigned to the symmetric –OH. The peaks at around 494 and 605 cm^{-1} are due to the Mn-O lattice vibrations [9]. The peaks at around 1858 and 2139 cm^{-1} are due to the C-C and C-CH_3 stretching modes. The peaks at around 1036 and 1558 cm^{-1} are assigned to the symmetrical C-N or N-CH_3. From the FTIR analysis it can observed that by increasing the pH of the solution reduces the amount of material absorbed for all the peaks appearing in the spectrum.

3.3 Photoluminescence

Figure 5(a) shows the PL spectra of the samples when excited at a 330 nm wavelength. At low pH (7.73), the emission spectrums depict a strong broad peak at around 376 nm. At high pH the PL spectra shows two peaks at around 376 and 420 nm. These emissions are associated with the transitions occurring within localized states in nanocrystalline structures [8]. The increase in broadness of the luminescence peak with an increase in the pH may be attributed to the increase in particle size, secondly it may be due to non-aggregated nanoflakes-like as confirmed by SEM and lastly may be due to the improvement of the crystallinity as the pH increased. The highest luminescence intensity is obtained at pH of 8.74. As shown in Figure 5(b), the Gaussian-multi curve fits of the broad peak with peaks at around 376 and 420 nm (red fit) and other peaks such as 373 (magenta fit) and 420 nm (blue fit) fits very well with the experimental curve of the MnO nanoflakes at pH solution of 9.01. These emissions may be ascribed to a high level transition in MnO semiconductors crystallites.

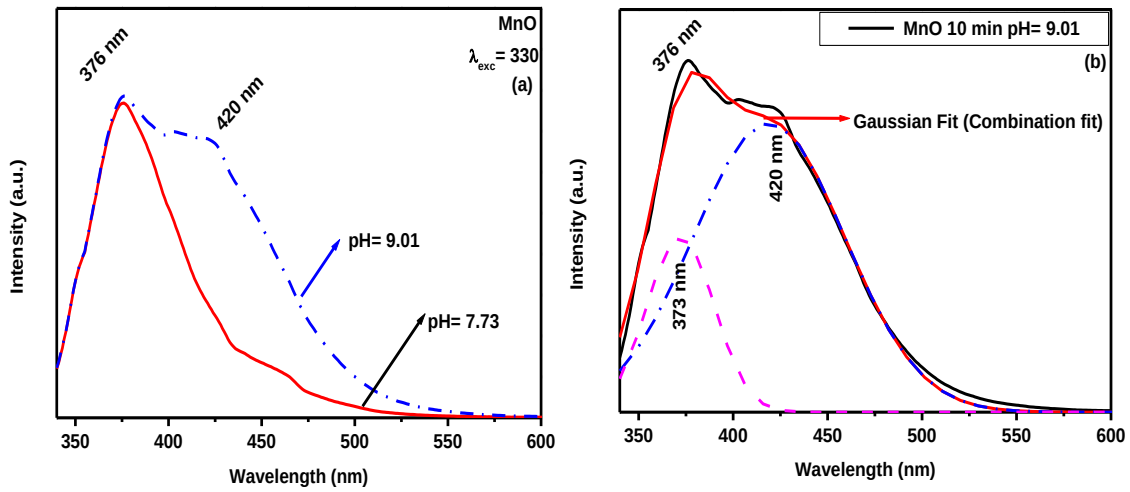

Figure 5. The PL spectra of MnO nanostructures prepared at (a) different pH and (b) a Gaussian fit of the 9.01 PL spectrum of the MnO nanoflakes-like prepared by the CBD method.

4. Conclusion

The MnO nanostructures have been successfully synthesized by the chemical bath deposition technique at 80°C. XRD showed that the structure of material is a monoclinic phase. EDS, XPS and FTIR confirmed the presence of the MnO nanostructures. PL showed that the emission spectra of the nanostructures depend on the pH. It was observed that the luminescence band become broad as the pH increased.

Acknowledgement

The author would like to acknowledge the National Research Foundation and Department of Science and Technology and the University of the Free State for financial support. We are also grateful to people currently of Centre for Microscopy at UFS for EDS, SEM, XPS, PL and X-ray diffraction measurements.

Reference

[1] Hu J, Odom T W and Lieber C M 1999 *Acc. Chem. Res.* **32** 435-455
[2] Dekker C, 1999 *Phys. Today* **52** 22-28
[3] Bredow T and Gerson R 2000 *Phys. Rev. B*. **61** 5194-5201
[4]Ntwaeabora O M, Kroon R E, Kumar V, Ahn J-P, Park J-K and Swart H C 2009 *J. of Phys and Chem of Solids* **70** 1438-1442.
[5] Cullity B D1978, *1956 Elements of X-ray Diffraction (2nd Ed), (Addison Wesley)* 285-284.
[6] Wagner C D, Riggs W M, Davis L E, Moulder J F and Muilenberg G E, 1979 *Handbook of X-ray photoemission spectroscopy, Perkin Elmer Corp. Publishers*,(Eden Prairie MN), 74-75.
[7] Shen X M and Clearfield J 1986 *J. Solid State Chem*. **64** 270-282
[8] Xiang X, Cheng X F, He S B, Yuan X D, Zheng W G, Li Z J, Liu C M, Zhou W L and Zu X T 2011 *Chin. Phys. B.* **20** 127801-2 to 127801-4
[9] Liping K, Menming Z, Zong-Huai L and Kenta O 2007 *Spectrochimica Acta Part A* **67** 864–869